



Double-sided self-pierce riveting with flat-bottom holes: a feasibility study

Luis M. Alves¹ · Rafael M. Afonso¹ · Patric T. Pereira¹ · Paulo A. F. Martins¹

Received: 20 July 2021 / Accepted: 28 September 2021 / Published online: 10 November 2021
© German Academic Society for Production Engineering (WGP) 2021

Abstract

This paper is focused on solving the problems of positioning and alignment of rivets in double-sided self-pierce riveting by means of flat-bottom holes that are previously machined in the overlapped sheets with greater mechanical strength. The work combines experimentation in joints made from dissimilar materials (aluminium AA5754-H111 and polyvinylchloride) with finite element modelling to investigate the influence of the flat-bottom hole geometry in the overall joining mechanisms. It is shown that the use of flat hole-bottom holes with rivets having identical chamfered angles in both ends is unable to create undercuts and to produce form-closed mechanical interlockings. Undercuts are created if different chamfered angles in the rivet ends are introduced to compensate the greater or lesser difficulty of the rivets to pierce through sheets with different mechanical strengths. Destructive shear and peel tests performed with different types of joints confirm the good performance of the joints produced by double-sided self-pierce riveting with flat-bottom holes.

Keywords Joining by forming · Double-sided self-pierce riveting · Flat-bottom holes · Experimentation · Finite element method

1 Introduction

Joining by forming makes use of plastic deformation to connect two or more elements of a mechanical component with appropriate ductility. The use of this technology has been growing rapidly in several industrial sectors, namely in the automotive [1] and aerospace [2] where many elements, sometimes made from dissimilar materials with very different strengths, are connected at ambient temperature.

The joining by forming technology is characterized by a set of different processes that are usually classified into two distinct groups: (1) joining by forming without auxiliary elements and (2) joining by forming with auxiliary

elements. The first group includes processes such as hemming, clinching, and cold pressure welding, in which the joints are obtained by single or combined action of the three-fundamental force-closed, form-closed, and material-closed joining mechanisms [3]. The second group requires the use of additional elements which, in general, promote the development of form-closed mechanisms (i.e., mechanical interlocking) and remain within the component after joining. Riveting and self-pierce riveting [4] are typical processes belonging to this second group and are commonly used to connect two or more overlapped elements.

The rapid growth in the use of self-pierce riveting (SPR) is due to several advantages against conventional riveting, such as: (1) the elimination of the need to pre-drill holes in the elements, (2) the suitability for applications where access from one side is limited, (3) the obtention of leak-proof joints and (4) the easiness of use and high productivity.

Still, there are several intrinsic disadvantages of SPR that cannot be forgotten, such as: (1) the application range limited to 1.5–4 mm of the total sheet thicknesses, (2) the positioning of thinner and/or softer sheets on the punch side, (3) the tearing up of the sheets placed on the punch side, and (4) the formation of material protrusions above and below the top and bottom sheet surfaces.

✉ Paulo A. F. Martins
pmartins@tecnico.ulisboa.pt

Luis M. Alves
luisalves@tecnico.ulisboa.pt

Rafael M. Afonso
rafael.afonso@tecnico.ulisboa.pt

Patric T. Pereira
patric.pereira@tecnico.ulisboa.pt

¹ IDMEC, Instituto Superior Técnico, Universidade de Lisboa, Av. Rovisco Pais, 1049-001 Lisbon, Portugal

The first attempt to overcome the above-mentioned disadvantages of SPR was done by Kato et al. [5], who redesigned the process to include a tubular rivet with chamfered ends in-between the sheets to be joined, which is subsequently pierced through the sheets in a single stroke. Flaring of the rivet ends during piercing ensures the creation of an undercut that holds the two overlapped sheets tightly together. The new process is shown in Fig. 1a and will be hereafter referred to as ‘conventional double-sided self-pierce riveting’, or simply ‘conventional DSSPR’ to emphasize the difference to SPR resulting from the utilization of semi-tubular instead of tubular rivets.

Subsequent developments by Huang et al. [6] allowed concluding that the advantages of conventional DSSPR of being independent from total sheet thicknesses and producing joints that are completely hidden inside the sheets came with the price of the joints being asymmetric whenever the rivets were incorrectly positioned and aligned with the sheets or when the rivets had obliquities resulting from their manufacturing process. New rivet geometries with outer [6] and inner flanges [7] placed at their mid tube height were proposed and their effectiveness in reducing the formation of asymmetric joints was demonstrated by means of numerical and experimental work with AA6063 aluminium sheets and AISI 304 stainless steel rivets.

Regardless of the advances that were achieved by all the above-mentioned investigations, the new process continued to experience difficulties with the positioning and alignment of the rivets and with its application to the joining of sheets made from dissimilar materials. The problem of joining dissimilar materials was firstly addressed by Alves et al. [8], who proposed a two-stroke variant of the original

DSSPR developed by Kato [5], in which the rivet is first forced through the sheet with greater mechanical strength, and then pressed through the softer sheet to obtain symmetric joints with good form-closed mechanical interlockings.

The development by Alves et al. [8] came after two preliminary studies by the same authors in monolithic overlapped joints made from AA5754-H111 aluminium sheets [9] and from polyvinylchloride (PVC) sheets [10], in which the authors concluded that typical chamfered angles $\alpha = 45^\circ$ can be made smaller or larger (say, $\alpha = 30^\circ$ or $\alpha = 60^\circ$) to compensate the greater or lesser difficulty of piercing through sheets with higher or lesser mechanical strength. However, like other authors, they also did not address the problem of the positioning and alignment of the rivets with the sheets in case of large, overlapped surfaces.

Under these circumstances the main goal of this paper is to solve the problem of the positioning and alignment of the rivets in DSSPR without compromising the overall performance of the resulting joints. The solution to be presented in this paper is based on preliminary machining (or forming) of a flat-bottom hole in the sheet with greater mechanical strength, in which the rivets are inserted before being pierced through the two sheets (Fig. 1b). Although the contribution to science and technology resulting from introducing a flat-bottom hole in a sheet may be questionable, it will be shown that the deformation mechanics of DSSPR changes in such a way that predominant form-closed joining by mechanical interlocking in the sheet with greater mechanical strength is replaced by a combination of form and force-closed joining. The latter is built-upon the radial pressure that is developed along the contact interface between the rivet and the flat-bottom hole after unloading.

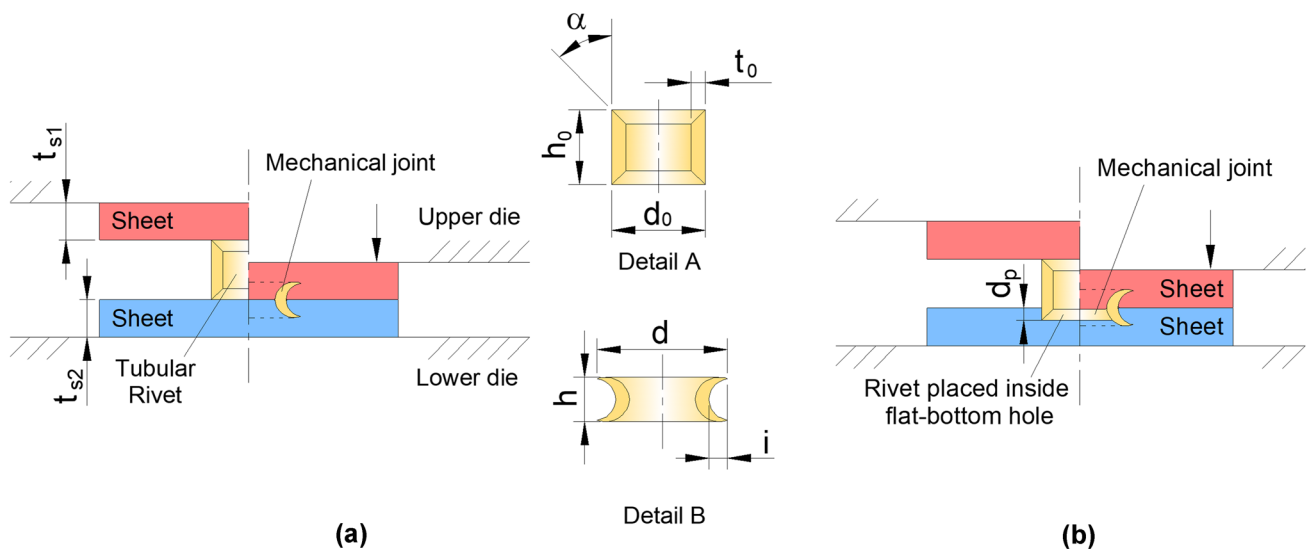


Fig. 1 **a** Conventional DSSPR with main notation and detail of the mechanical interlocking and **b** the new proposed DSSPR with flat-bottom hole showing the geometries at the beginning and end of joining

The effectiveness of the proposed solution is demonstrated by means of a numerical and experimental investigation that was carried out in sheets made from dissimilar materials (AA5754-H111 aluminium and PVC) with AISI 304 stainless steel tubular rivets. Results demonstrate the advantages of using different chamfered angles in the rivet ends to compensate the greater or lesser difficulty of the rivets to pierce through sheets and to obtain a combined form and force-closed joint. Destructive peel and shear tests included at the end of the paper show that joints produced by DSSPR with a flat-bottom hole have better performance than those produced by conventional DSSPR.

2 Methods and procedures

2.1 Materials and flow curves

The investigation was performed in dissimilar lap joints made from commercial AA5754-H111 aluminium and polyvinylchloride (PVC) sheets with 5 mm thickness. The chamfered tubular rivets were made from AISI 304 stainless steel tubes with an outer diameter of 10 mm and a wall thickness of 1.5 mm.

The flow curves of the materials were retrieved from previous works of the authors on DSSPR of AA5754-H111 aluminium and polyvinylchloride (PVC) sheets [8] and involved the use of tensile and stack compression tests. The tests were carried out at ambient temperature in a hydraulic testing machine (Instron SATEC 1200 kN) with a crosshead speed of 5 mm/min and the resulting flow curves are shown in Fig. 2.

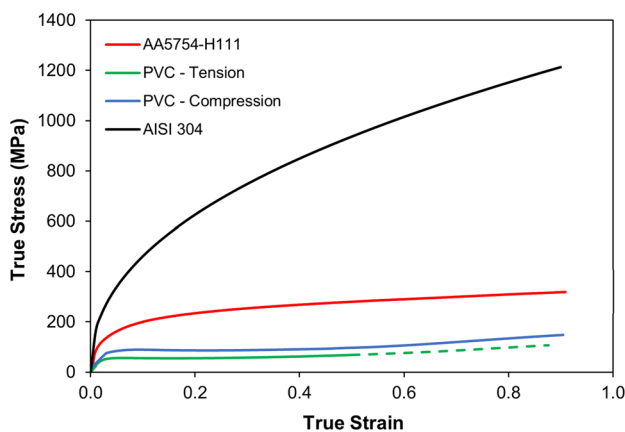


Fig. 2 Flow curves of the aluminium AA5754-H111 and polyvinylchloride (PVC) sheets and of the AISI 304 stainless-steel tubes

2.2 Workplan

Previous work on conventional DSSPR allowed identifying the main process parameters and joining mechanisms. The parameters are duly indicated in Fig. 1a as: (1) the upper and lower sheet thicknesses t_{si} , and (2) the outer diameter d_0 , (3) the height h_0 , (4) the wall thickness t_0 , (5) the chamfered angles α_i of the rivet ends and (6) the depth d_p of the flat-bottom hole (refer to Fig. 1b).

The main differences between the conventional and new proposed variant of DSSPR are the utilization of flat-bottom holes and chamfered angles α_i with different values in both rivet ends. For this reason, and to avoid repeating previous work of the authors, the focus of this paper is solely placed on the depth d_p of the flat-bottom holes and in the values of the chamfered angles α_i (Fig. 1).

The experiments were carried out at ambient temperature with a crosshead speed of 5 mm/min in the same hydraulic testing machine where the flow stresses had been previously obtained. The following procedure was utilized:

1. Cut out the sheet specimens and the tubular rivet from the supplied materials,
2. Machining the chamfered angles α_i of the rivet ends,
3. Machining a flat-bottom hole in the aluminium sheet,
4. Positioning the rivet in the flat-bottom hole,
5. Placing the PVC sheet on top of the rivet as shown in Fig. 1b,
6. Compressing the PVC sheet against the rivet until contact between the two sheets,
7. Cutting the test specimen along its cross-sectional plane to observe the joint and to measure the interlocking distances or,
8. Performing shear and peel destructive tests to evaluate and compare the performance of the joints.

Whenever necessary to explain the changes in the deformation and joining mechanics introduced by the new proposed DSSPR, comparisons were made against conventional

Table 1 Summary of the process operating parameters used in the experimental and numerical tests with the new proposed double-sided self-pierce riveting with flat-bottom hole (Fig. 1)

| Rivet | | | | |
|-------------|---------------|------------|------------|--------------|
| Material | d_0 (mm) | h_0 (mm) | t_0 (mm) | α (°) |
| AISI 304 | 10 | 8 | 1.5 | 30, 45, 60 |
| Sheets | | | | |
| Material | t_{si} (mm) | d_p (mm) | d_0 (mm) | |
| AA5754-H111 | 5 | 1, 2, 4 | 10 | |
| PVC | 5 | – | – | |

DSSPR. Table 1 summarizes the work plan that was designed to accomplish the above-mentioned research objectives. At least five different test samples were utilized for each set of operating parameters.

2.3 Numerical modelling

Numerical modelling of the new DSSPR with flat-bottom hole was performed with the in-house finite element software i-form [11] based on the modified weak form of the quasi-static force equilibrium equations to include contact and sliding with friction between deformable objects,

$$\int_V \sigma'_{ij} \delta D_{ij} dV + \int_V \sigma_m \delta D_v dV - \int_{S_i} t_i \delta u_i dS + \int_{S_f} \left(\int_0^{|u_r|} \tau_f \delta u_r \right) dS + K_1 \sum_{c=1}^{N_c} g_n^c \delta g_n^c = 0 \quad (1)$$

The software is built upon the flow formulation and employs a control volume approach with velocities u_i as the primary unknowns. Other symbols in (1) are the deviatoric Cauchy stress σ'_{ij} , the hydrostatic stress σ_m , the rate of deformation D_{ij} , the volumetric rate of deformation D_v , the tractions t_i applied on the boundary S_i of the control volume and

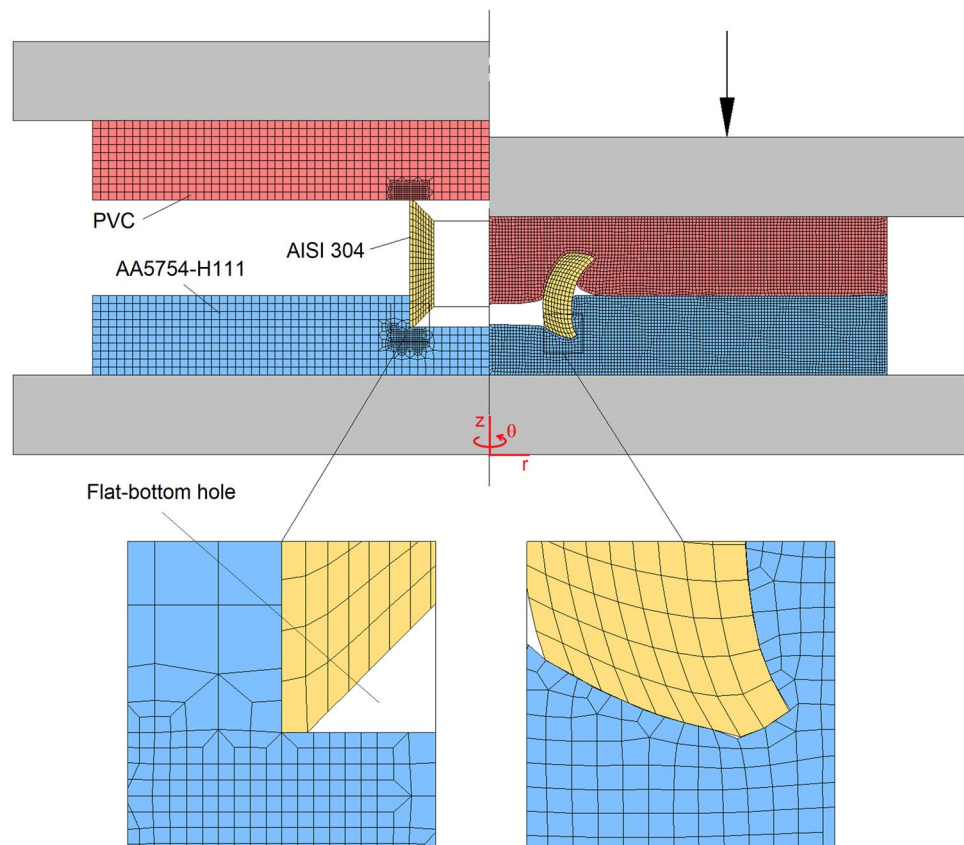
the friction shear stress τ_f and the relative sliding velocity u_r on the contact interfaces S_f between deformable and rigid objects.

The last term of (1) accounts for the contact between deformable objects by means of a two-pass contact search algorithm in which the N_c contact pairs are automatically extracted from the faces of the finite elements utilized in the discretization. The symbol g_n^c stands for the normal gap velocities in the contact pairs, which are penalized by a large number K_1 to avoid penetration. Details are given in Nielsen and Martins [12].

Figure 3 shows a typical finite element model utilized in the numerical simulation of the DSSPR with a flat-bottom hole at the beginning and end of joining. The model considered the plastically deforming region of the objects to be axisymmetric and discretized the longitudinal cross-section of the deformable objects (sheets and rivets) by means of quadrilateral elements. Several remeshings were carried out to repair and refine the mesh as the rivet is forced through the sheets. The tools were modelled as rigid objects and their contours were discretized by means of linear contact-friction elements.

The computational time for a typical analysis using a convergence criterion for the velocity and force equal to 10^{-3}

Fig. 3 Typical finite element model at the beginning and end of joining by double-sided self-pierce riveting with a flat-bottom hole ($d_p = 2$ mm, $\alpha_{alu} = 45^\circ$, $\alpha_{pvc} = 45^\circ$)



was approximately 15 min. on a computer equipped with an Intel i7-5930K CPU processor.

3 Results and discussion

3.1 Joining mechanisms

The utilization of flat-bottom holes for positioning and aligning the rivets is likely to change material flow in both the rivets and the neighbouring sheet materials. How relevant are these changes? Will the form-closed mechanisms of conventional DSSPR still prevail when flat-bottom holes are machined in the sheets with greater mechanical strength? What is the influence of these changes in the overall mechanical performance of the joints?

Figure 4 helps answering these questions by disclosing the experimental and finite element predicted cross-sections of dissimilar lap joints made from AA5754-H111 aluminium and PVC that were produced by conventional DSSPR and by the new proposed DSSPR with flat-bottom holes. As seen in Fig. 4a, b, the new proposed DSSPR reduces the amount of unfilled volume between the lower aluminium sheet and the outer rivet wall that is observed in conventional DSSPR (refer to the black circle in the left-side detail of Fig. 4c).

The final unfilled volume in conventional DSSPR results from elastic unloading, which forces the sheet materials to move inwards, and the rivet ends to curl for compensating the constraint caused by the contact between the two

sheets at the joint centre (refer to the arrows in the left-side detail of Fig. 4c for details on the movement of PVC during unloading).

Conversely, the results included in Fig. 4b and in the right-side detail of Fig. 4c, also allow understanding the role of the gap created by the flat-bottom hole in accommodating the elastic recovery and diminishing the upward movement of PVC during unloading. This explains the reason why the protrusions on the upper surface of the PVC sheets are smaller than those produced by conventional DSSPR (Fig. 4c).

In connection to what was said above, it is worth mentioning that the differences observed between the experimental and numerically predicted protrusions of Fig. 4 are due to the elimination of the circumferential constrain when halving the specimens lengthwise to reveal their cross-sections. This elimination is not taken into consideration in finite element modelling.

Regarding the question on the possibility of maintaining the form-closed mechanism that is observed in conventional DSSPR, results in Fig. 4b and in the right-side detail of Fig. 4c indicate that the mechanical interlocking between the rivet and the aluminium sheet almost vanishes. In other words, the form-closed mechanism of conventional DSSPR disappears and joining is exclusively ensured by a force-closed mechanism built upon the residual normal pressures (radial stresses, σ_r) that are created on the contact interface between the rivet and the aluminium sheet at the end of joining (i.e., after unloading). The form-closed mechanism

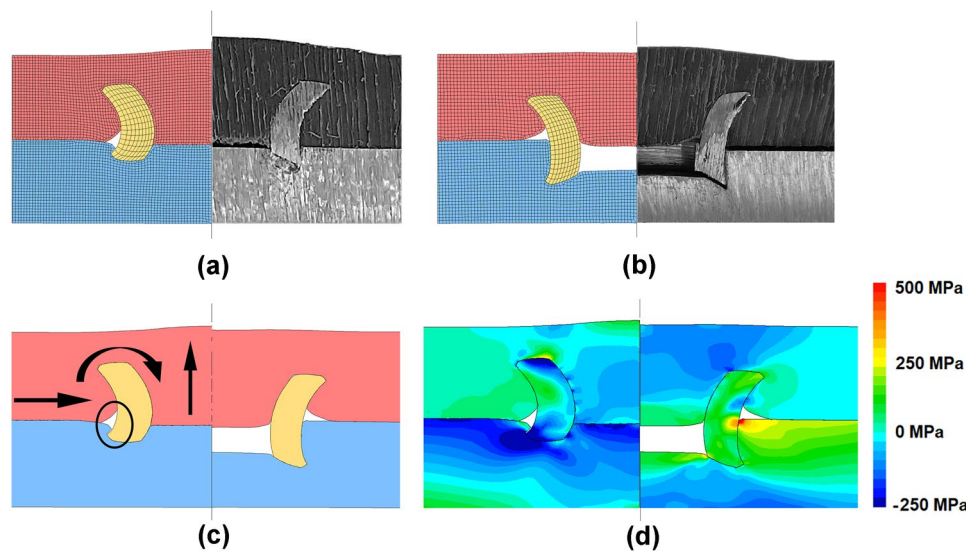


Fig. 4 Double-sided self-pierce riveting (DSSPR) of AA5754-H111 aluminium and PVC sheets with AISI 304 stainless-steel rivets having chamfered angles equal to 45° at both ends. **a** Finite element predicted geometry and photograph of the cross section after elastic recovery for conventional DSSPR. **b** Finite element predicted geom-

etry and photograph of the cross section after elastic recovery for DSSPR with a flat-bottom hole ($d_p = 2$ mm). **c** Detail of the joints produced in **a**, **b**. **d** Finite element predicted distribution of radial stress σ_r (MPa) after elastic recovery for (left) conventional DSSPR and (right) DSSPR with a flat-bottom hole

only prevails in the PVC sheets due to the formation of large undercuts between the rivet and the sheet (Fig. 4b).

Figure 4d shows the finite element predicted distributions of residual stress σ_r , for the conventional and new DSSPR with a flat-bottom hole. As seen, compressive residual stresses σ_r are found to occur along the inner rivet wall-aluminium sheet contact interface of conventional DSSPR (Fig. 4d-left), meaning that the rivet is subjected against the aluminium sheet after unloading. In contrast, the residual stresses along the outer rivet wall are negligible because this surface is free due to the previously mentioned unfilled volume between the aluminium sheet and the outer rivet wall.

The distribution of residual stresses in the new DSSPR with a flat-bottom hole (Fig. 4d-right) shows tensile values along the contact interface between the outer rivet wall and the aluminium sheet, meaning that the rivet is subjected against the flat-bottom hole wall after unloading. Because there is no undercut, the resulting joining mechanism between the rivet and the aluminium sheet is essentially force-closed based.

The residual stresses σ_r acting along the contact interface between the rivet and the aluminium sheet prevent tangential movement due to friction and help keeping the overlapped

aluminium and PVC sheets together. As will be seen in the destructive tests, the large contact interfaces of the new proposed DSSPR with a flat-bottom hole are responsible for an increase in the overall mechanical performance of these joints compared to those produced by conventional DSSPR.

The changes in the above-mentioned joining mechanisms gives rise to two main differences in the force vs. displacement evolutions shown in Fig. 5. First, the required forces to pierce the rivets through the sheets are greater in conventional DSSPR (37 kN) than in the new DSSPR (27 kN). The sudden increase in force above these values is caused by attaining full contact between the compression platen and the upper sheet surfaces (refer, for example, to the process insets of the new DSSPR with a flat-bottom hole that are included in the graphic).

Second, the differences in the maximum displacement are due to the smaller free height of the rivets that are placed inside the flat-bottom holes of the new DSSPR.

This discussion around the joining mechanisms inevitably leads to the question of whether it will be worthwhile to reduce or increase the depth of the flat-bottom holes to recover the mechanical interlocking in the aluminium sheets, and to improve the capability of the joints to withstand destructive peel and shear forces. The answer to this question will be given in the following section.

3.2 Depth of the flat-bottom holes

The sensitivity of the joints produced by means of the new DSSPR to the geometry of the flat-bottom holes was examined by varying (decreasing and increasing) their depth d_p while keeping the material and size of sheets and rivets unchanged. The results of this sensitivity analysis are summarized in Fig. 6.

As can be observed, the variation in the hole depth d_p does not produce changes in the joining mechanism because no significant undercuts are created between the rivets and the aluminium sheets. In fact, when the depth $d_p = 1$ mm, the rivet is mainly pierced through the softer PVC sheet until the vicinity of the upper sheet surface (Fig. 6a). A very large and wide protrusion is formed.

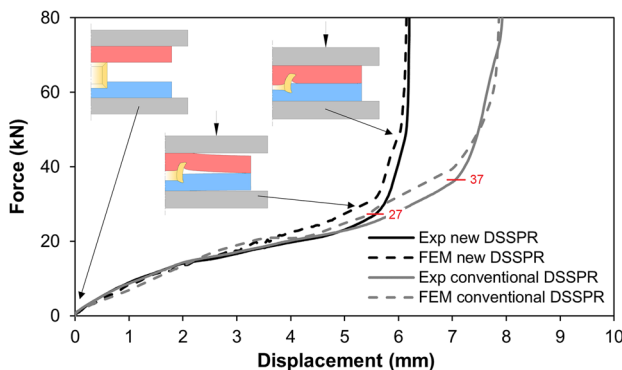


Fig. 5 Experimental and finite element predicted evolution of the riveting force with displacement for the conventional and new DSSPR with a flat-bottom hole ($d_p = 2$ mm) in case of joining AA5754-H111 aluminium and PVC sheets with AISI 304 stainless-steel rivets ($\alpha = 45^\circ$)

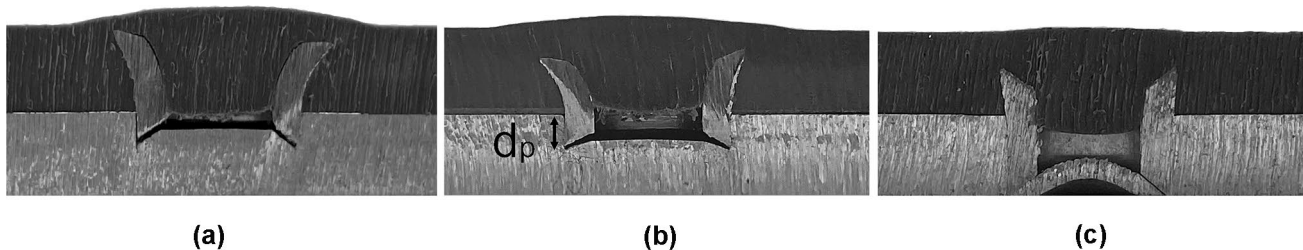


Fig. 6 Sensitivity of the joints to the depth **a** $d_p = 1$ mm, **b** $d_p = 2$ mm and **c** $d_p = 4$ mm of the flat-bottom holes in case of joining AA5754-H111 aluminium and PVC sheets with AISI 304 stainless-steel rivets having chamfered angles equal to 45° at both ends

In contrast, when the depth $d_p = 4$ mm, the rivet is pierced all through the aluminium sheet and creates a central disk that buckles under radial edge compression applied by the chamfered tube end (Fig. 6c).

The above-mentioned results justify the utilization of depth d_p values in the range of 2 mm (i.e., 40% of the total sheet thickness, Fig. 6b), but this conclusion does not have any effect in the attempt to create undercuts and to recover the mechanical interlocking between the rivets and the aluminium sheets.

3.3 Chamfered rivet ends

The solution to recover the mechanical interlocking in DSSPR with a flat-bottom hole involves the use of different chamfered angles in the rivet ends to account for the greater or lesser difficulty of piercing through sheets with higher or lesser mechanical strength. In practical terms, this means extending the strategy that Alves et al. [8] previously applied in conventional DSSPR to create form-closed joints in DSSPR with flat-bottom holes.

The result is shown in Fig. 7 for a test case using different chamfered angles at the rivet ends ($\alpha_{Alu} = 60^\circ$ and $\alpha_{PVC} = 30^\circ$). Experimental measurements of the undercuts in the aluminium and PVC sheets provide values of 0.33 mm and 0.88 mm, respectively. The results are similar to those obtained by finite elements (0.41 mm and 0.83 mm) and demonstrate that it is possible to obtain a combined form and force-closed joint in DSSPR with flat-bottom holes, if different chamfered angles are machined at the rivet ends.

In connection to the result shown in Fig. 7 it is worth noticing that no significant undercuts were found to exist between the rivets and the aluminium sheets for the test cases shown in Fig. 6, in which identical chamfered angles $\alpha_{Alu} = \alpha_{PVC} = 45^\circ$ were utilized at the rivet ends.

3.4 Destructive peel and shear testing

The importance of having a mechanical interlocking in the aluminium sheet is demonstrated by analysing the results of the destructive tests carried out in joints produced by the conventional DSSPR and the new DSSPR with flat-bottom holes using identical ($\alpha_{Alu} = \alpha_{PVC} = 45^\circ$) and different ($\alpha_{Alu} = 60^\circ, \alpha_{PVC} = 30^\circ$) chamfered angles at the rivet ends.

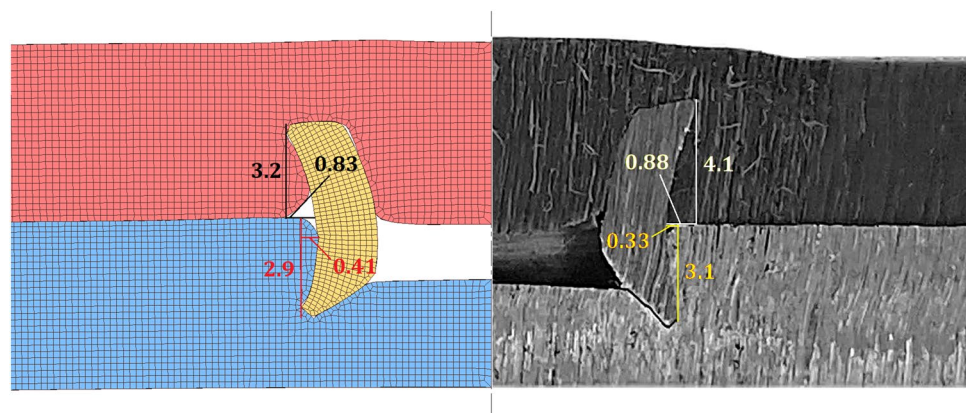
The experimental force vs. displacement evolutions shown in Fig. 8a are the average results obtained for the test samples utilized for each type of joint. Standard deviations are in the range of 0.5 to 0.6 and indicate good repeatability of the results.

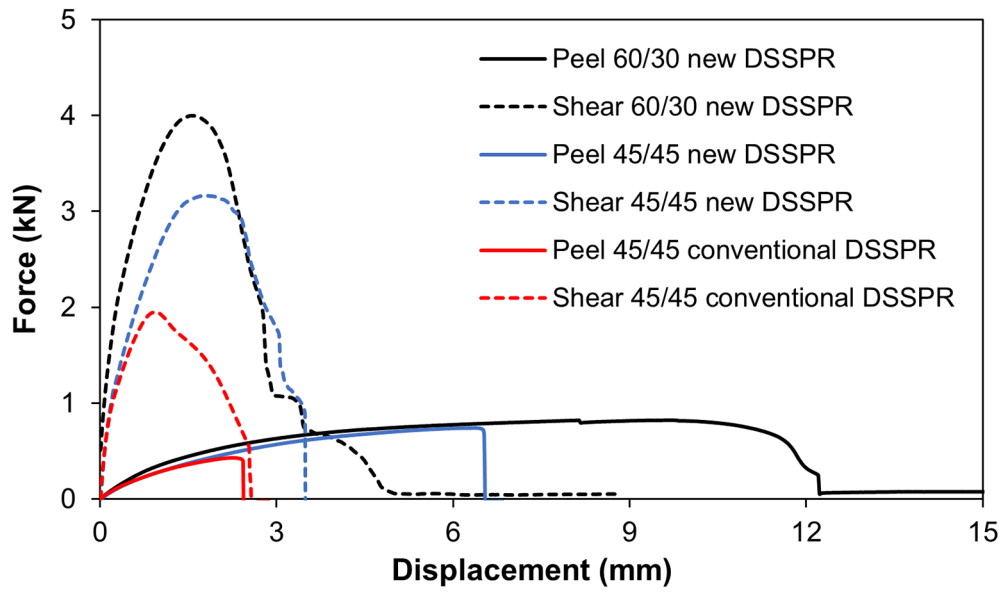
Two main conclusions can be derived from Fig. 8a. First, the shear strength of the joints produced by the new DSSPR using rivets with different chamfered angles at failure is the greatest (4 kN, refer to the peak value in the black dashed curve of Fig. 8a), and equal to twice of the joints produced by conventional DSSPR. This result is attributed to the combined action of the undercut in the aluminium sheet plus friction on the rivet-hole contact interface, which opposes detachment and dragging out of the rivet by shear. In fact, the rivet-hole contact interface provides values in the range of 3.1 mm (Fig. 7), in contrast with an almost absence of contact interface in conventional DSSPR (refer also to Fig. 4a).

In what concerns the resistance to failure by peeling, greater values are once again obtained for the joints produced by the new DSSPR with rivets having different chamfered angles (refer to the back solid curve in Fig. 8a). However, in this case is not the increase in the maximum force that is relevant, (because forces are similar), but the total amount of displacement that the joints can safely withstand before failing.

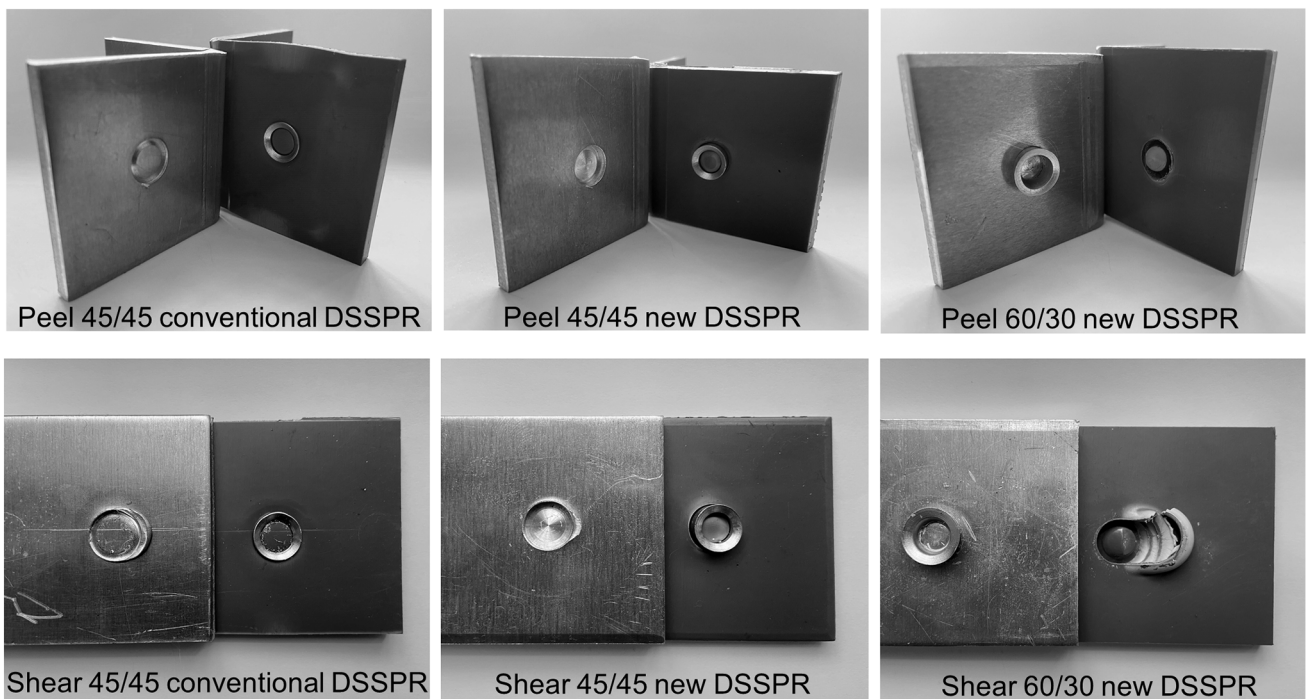
The combined action of the undercut in the aluminium sheet plus the frictional resistance along the rivet-hole contact interface justify the greater performance of the joints produced by the new DSSPR with flat-bottom holes using rivets with different chamfered angles. A closer look at the

Fig. 7 Finite element and photograph of a cross-sectional joint made from AA5754-H111 aluminium and PVC sheets with AISI 304 stainless-steel rivets having different chamfered angles $\alpha_{Alu} = 60^\circ$ and $\alpha_{PVC} = 30^\circ$ ($d_p = 2$ mm)





(a)



(b)

Fig. 8 **a** Destructive peel and shear forces vs. displacement for overlapped joints made from AA5754-H111 aluminium and PVC sheets that were assembled with AISI 304 stainless-steel rivets by means of

the conventional and the new DSSPR with flat-bottom holes. **b** Photographs of the different types of specimens after testing

photographs included in Fig. 8b allows concluding that this type of joint (refer to the upper rightmost pictures) is the only having the rivets fixed to the aluminium sheets after finishing the peel and shear tests. All the other joints have the rivet fixed to the PVC sheets.

4 Conclusions

Positioning and alignment of the rivets in double-sided self-pierce riveting (DSSPR) can be solved by machining flat-bottom holes in the sheets with greater mechanical strength. The geometry of the flat-bottom holes regardless of their depth tends to modify the predominant form-closed mechanism of conventional DSSPR into a predominant force-closed mechanism, in which the friction forces acting along the rivet-hole interfaces in the sheets with greater mechanical strength are responsible for keeping the overlapped sheets together.

The use of rivets with different chamfered angles (say, 30° and 60°) to compensate the greater or lesser difficulty of the rivets to pierce through sheets with different mechanical strengths, allows enhancing the forced-closed mechanisms by creation of good undercuts (mechanical interlockings) between the rivets and the aluminium sheets.

The new joints produced by DSSPR with flat-bottom holes and making use of rivets with different chamfered angles provide the best shear and peel test performances with maximum forces respectively equal to 4 kN and 0.8 kN. In particular, the shear strength is twice of that of the joints produced by conventional DSSPR.

Future developments in DSSPR with flat-bottom holes will be focused on the utilization of thinner dissimilar sheets and smaller tubular rivets with different ratios between the outer diameter and the wall thickness.

Acknowledgements The authors would like to thank the support provided by Fundação para a Ciência e a Tecnologia of Portugal and IDMEC under LAETA-UIDB/50022/2020.

Author contributions LMA: Conceptualization, Investigation, Methodology, Experimentation, Writing -editing. RMA: Investigation, Experimentation, Visualization, Writing -editing. PTP: Numerical Modelling, Visualization. PAFM: Funding acquisition, Methodology, Numerical Modelling, Supervision, Writing—original draft.

Funding The research was supported by Fundação para a Ciência e a Tecnologia of Portugal and IDMEC under LAETA- UIDB/50022/2020.

Availability of data and materials Authors confirm that the data and material supporting the findings of this work are available within the article.

Code availability Not applicable.

Declarations

Conflict of interest The authors have no competing interests or conflicts of interest to declare that are relevant to the contents of this article.

Ethical approval The article follows the guidelines of the Committee on Publication Ethics (COPE) and involves no studies on human or animal subjects.

Consent to participate Not applicable.

Consent for publication Not applicable.

References

- Meschut G, Janzen V, Olfermann T (2014) Innovative and highly productive joining technologies for multi-material lightweight car body structures. *J Mater Eng Perform* 25:1515–1523
- Johnson P (2020) Quality control and nondestructive testing of self-piercing riveted joints in aerospace and other applications. In: Chaturvedi M (ed) *Welding and joining of aerospace materials*. Woodhead Publishing, UK
- Groche P, Wohletz S, Brenneis M, Pabst C, Resch F (2014) Joining by forming—a review on joint mechanisms, applications and future trends. *J Mater Process Technol* 214:1972–1994
- Li D, Chrysanthou A, Patel I, Williams G (2017) Self-piercing riveting—a review. *Int J Adv Manuf Technol* 92:1777–1824
- Kato K, Okamoto M, Yasuhara T (2001) Method of joining sheets by using new type of rivets. *J Mater Process Technol* 111:198–203
- Huang Z, Yao Q, Lai J, Zhao J, Jiang Z (2017) Developing a self-piercing riveting with flange pipe rivet joining aluminium sheets. *Int J Adv Manuf Technol* 91:2315–2328
- Huang Z, Xue S, Lai J, Xia L, Zhan J (2014) Self-piercing riveting with inner flange pipe rivet. *Proc Eng* 81:2042–2047
- Alves LM, Afonso RM, Pereira PT, Martins PAF (2021) Double-sided self-pierce riveting of dissimilar materials. *Int J Adv Manuf Technol*. <https://doi.org/10.1007/s00170-021-07426-3>
- Alves LM, Afonso RM, Martins PAF (2020) Double-sided self-pierce riveting. *Int J Adv Manuf Technol* 108:1541–1549
- Alves LM, Afonso RM, Martins PAF (2021) Double-sided self-pierce riveting of polymer sheets. *J Adv Joining Proc* 3:100051
- Nielsen CV, Zhang W, Alves LM, Bay N, Martins PAF (2013) Coupled finite element flow formulation. In: Davim JP (ed) *Modelling of thermo-electro-mechanical manufacturing processes with applications in metal forming and resistance welding*. Springer, New York. https://doi.org/10.1007/978-1-4471-4643-8_3
- Nielsen CV, Martins PAF. (2021) Finite element simulation: a user's perspective In: *Metal forming: formability, simulation and tool design*. Academic Press, London. <https://doi.org/10.1016/B978-0-323-85255-5.00011-X>

Publisher's Note Springer Nature remains neutral with regard to jurisdictional claims in published maps and institutional affiliations.